# NEUTRON DIFFRACTION CHARACTERIZATION
# OF RESIDUAL STRAIN IN WELDED INCONEL 718
# FOR NASA SPACE SHUTTLE FLOW LINERS

C.R. Rathod[1], V. Livescu[2], B. Clausen[2], M.A.M. Bourke[2],
W.U. Notardonato[3], M. Femminineo[3], and R. Vaidyanathan[1]

[1]University of Central Florida
Orlando, Florida, 32816, USA

[2]Los Alamos National Laboratory
Los Alamos, New Mexico, 87545, USA

[3]NASA Kennedy Space Center
Kennedy Space Center, Florida, 32899, USA

## ABSTRACT

This work quantitatively assesses residual strains and stresses associated with the weld repair process used to repair cracks on NASA's space shuttle flow liners. The coupons used in this investigation were made of the same INCONEL 718 alloy used for the flow liners. They were subjected to identical welding and certification procedures that were carried out on the space shuttle. Neutron diffraction measurements at Los Alamos National Laboratory determined residual strains at selected locations in a welded coupon at 293 K and 135 K. The weld repair process introduced Mises effective residual stresses of up to 555 MPa. On comparing the measurements at 293 K and 135 K, no significant change to the residual strain profile was noted at the low temperature. This indicated minimal mismatch in the coefficients of thermal expansion between the base metal and the weld.

## INTRODUCTION

The space shuttle main propulsion system delivers liquid hydrogen and liquid oxygen through twelve-inch diameter feedlines to the three main engines at roughly 75 Kg/sec and 445 Kg/sec, respectively, during ascent. Each of the six feedlines has three bellowed articulating joints to allow flexing due to thermal transients and flow forces. Two of the three joints are supported internally with a ball strut tie rod assembly, but the joint closest to the engine is supported externally with a heavier gimbal joint to avoid flow disturbance
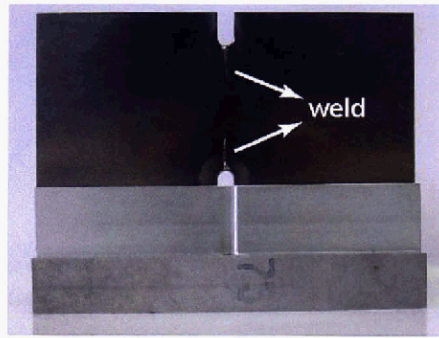
|  | (a) |  | (b) |

**FIGURE 1. (a)** An INCONEL 718 flow liner that is currently used on NASA space shuttles Discovery, Atlantis and Endeavor. **(b)** A coupon with welds propagating vertically from each notch in an aluminum holder.

prior to entering the engine's low pressure pump impellers. To meet the 100-mission life requirement for these feedlines, flow induced high cycle fatigue of the line bellows must be prevented. That is the purpose of flow liners that shield the bellows on the inside of the line from direct flow. The flow liner consists of an upstream and downstream section, which are independently welded to the inside of the feedline at either side of the bellows to provide independent motion as the line flexes. Both flow liner sections have elongated slots 6.35 mm wide to maintain an equal pressure between the rearside of the liner and the flow stream as well as to aid in cleaning of the bellow area during manufacture. Columbia's flow liners were made of CRES 321 with 76 slots per section, while the subsequently built Discovery, Atlantis, and Endeavour have INCONEL 718 liners (see FIGURE 1a) with 38 slots per section.

In the summer of 2002, the space shuttle fleet was grounded when cracks were discovered in the liquid hydrogen feedline flow liners nearest the engine interface on all four orbiters. No cracks were seen on any of the liquid oxygen flow liners. All the cracks originated at the high stress areas where the straight portion of the slot transitioned to the semicircular curved area or at the center of the semicircular area itself. On the 4 orbiters there were a total of 11 cracks with 9 on downstream sections and 2 on upstream sections. The longest crack was 8.38 mm long. No cracking issues have been seen on any of the flex joints further upstream.

An intensive effort to understand the cause of these cracks ensued. Part of the problem was in the manufacture of the liners themselves. The slots were punched out with a press and microcracks remained around the slots from this process. Also, the blade pass frequency of the low pressure fuel turbopump (which is just inches downstream of the flow liner) while running at main stage thrust levels roughly matched the natural frequency of the flow liner. Clearance between the impeller blades and pump housing allowed slight leakage which flowed back upstream along the feedline wall. This in turn excited the flow liner as the frequencies matched. This effect extended upstream for a couple line diameters, but was enough to reach the gimbal joint near the engine interface.

Several repair options were investigated. With a great deal of research and testing, a method was developed to return nearly all of the original strength to the part. It involved a several stage welding process. United Space Alliance (USA) welders processed INCONEL 718 and CRES 321 sample coupons that were supplied with high and low cycle fatigue induced cracks in them. These fabricated coupons were subsequently subjected to gas tungsten arc welding. This type of welding is typically used for oxygen sensitive materials and produces no slag after the weld pass. After welding they were tested to failure. Non-

destructive evaluation techniques including x-ray, eddy current, and ultrasound were used to verify acceptable welds. After the certification process was complete, USA applied the same procedure to the cracks in the orbiters. In order to prevent future occurrences of cracks, a process to eliminate the microcracks in the rest of the slots was developed. It involved a hand polishing operation that removed a minimal amount of material. This too was successfully tested. To date these repairs and improvements have been incorporated on all the orbiters. Atlantis and Endeavour have since flown and the flow liners subsequently inspected. No new cracks or damage to the weld repairs were noted.

This work was initiated to quantitatively assess the residual strains and stresses associated with the aforementioned weld repair process. Consequently, the coupons used in this investigation were made of the same INCONEL 718 alloy used for the flow liners and subjected to identical welding and certification procedures that were carried out on the space shuttle (again by the same team of USA welders). Neutron diffraction measurements were carried out at Los Alamos National Laboratory to determine residual strains at selected locations in a welded coupon at ambient and cryogenic temperatures. The neutron diffraction technique uses the atomic planes in specimens as internal strain gauges [1]. The distances between atomic planes, directly obtained from diffraction spectra at different locations, can then be used to map residual strain profiles (e.g., [2]). While such measurements are regularly performed in open environments at room temperature, making them at elevated or cryogenic temperatures in vacuum environments require additional engineering. Neutrons have a greater penetration depth than conventional x-rays and allow specimens to be placed in controlled-environment chambers and aligned so that the neutron beam can penetrate through the chamber and diffract from the specimen. Furthermore, the larger penetration depth of neutrons results in measurements being representative of the bulk through-thickness (for the case of these coupons) rather than the surface.

An aluminum vacuum chamber with a copper cold mass cooled by liquid nitrogen was fabricated to cool coupons while allowing for the simultaneous acquisition of neutron diffraction spectra. This chamber was installed in the Spectrometer for Materials Research at Temperature and Stress (SMARTS) at Los Alamos National Laboratory (LANL) [3]. Neutron diffraction spectra from the coupons were obtained at 135 K. While this temperature was above the coldest operating temperature of the flow liner (which carry liquid hydrogen at 23 K), it was nevertheless deemed useful to gauge the effect of a 153 K drop in temperature on the residual strain field due to the weld repair procedure.


## EXPERIMENTAL

### Coupon Preparation

Eight INCONEL 718 test coupons were fabricated at NASA Marshall Space Flight Center (MSFC). The same fabrication method that was used for the weld qualification process prior to welding the flight element cracks was used here. The coupons had a section length and width of 152.4 mm by 50.8 mm, respectively, and were approximately 1.27 mm thick. Each coupon had two half slots at the top and bottom, as shown in FIGURE 1b. The coupons were fatigue cycled (at approximately 15 Hz) at NASA MSFC. The test coupons were then shipped to NASA Kennedy Space Center (KSC) for weld repair of the cracks. The coupons were repaired using the same gas tungsten arc welding process that was completed on the flight elements. This weld process was (a) prepare the slots for welding with a cutting tool, (b) weld the crack with INCONEL 718 filler and run a feather pass along the toe of the weld, both sides, (c) grind the weld flush, prepare slot for

169

**TABLE 1.** Specifications of the coupons used in this investigation (fabricated at NASA Marshall Space Flight Center).

| Specimen | Net section width | Thickness | Net section stress | Cycles | | Final crack length |
|----------|-------------------|-----------|--------------------|--------|--------|--------------------|
| | (mm) | (mm) | (MPa) | Fatigue | To final crack length | (mm) |
| RS1 | 51.03 | 1.27 | control | | | none |
| RS3 | 50.98 | 1.27 | 206.84 | 100,000 | | none |
| RS5 | 51.03 | 1.24 | 206.84 | | 325,000 | 10.41 |

the autogenous heat pass (no filler material), (d) non-destructive inspection - 10x to 30x visual, eddy current, ultrasonic and x-ray, (e) weld autogenous pass inside of the slot, and (f) polish the weld and slot. Three coupons were selected for this investigation and are described in TABLE 1.

## Cryogenic Test Chamber

To minimize the temperature gradient across the coupon due to convective heat losses and prevent the accumulation of ice on the sample, the coupon was cooled while in a vacuum. This was accomplished by holding the coupon in a fixture in an aluminum chamber. The fixture was a rectangular frame that held the coupon and was in thermal contact with a "cold mass" at the bottom of the chamber. Care was taken to ensure that By controlling the flow of liquid nitrogen through the "cold mass", the temperature of the coupon was controlled. Due to a leak from the cold mass, the vacuum fluctuated between 10-500 mTorr. The description of this chamber and the test setup are forthcoming [4-6].

## Neutron Diffraction

Neutron diffraction measurements were performed on SMARTS at Los Alamos Neutron Science Center (LANSCE) at LANL. A "time-of-flight" neutron beam with a cross-section of 2 X 2 mm was used for residual strain measurements at room temperature (293 K) and at 135 K, in a spatially resolved mode. While the room temperature measurements were performed under ambient conditions, the cryogenic measurements were made in the aforementioned cryogenic test chamber. For both cases, the coupon was placed on a computer controlled XYZ-theta stage, so that any desired point on the sample could be examined during the experiment. This was achieved with the aid of two Leica theodolites that, by triangulation, could locate a sample with an accuracy of 0.1 mm.

FIGURE 2a shows how the orientation of the incident neutron beam relative to the coupon dictates the direction of the measured strain. For each orientation, strain information is obtained for two directions (since two banks of detectors that were 180° apart were used). Horizontal placement of the coupon at 45° to the incident beam provided strain information in the in-plane longitudinal or x direction and the through-thickness or z direction. Vertical placement of the coupon at 45° to the incident beam provided strain information in the in-plane transverse or y direction and the through-thickness or z direction. FIGURE 2b shows the locations of the measurements. The average neutron count time per location was 9 minutes although count times as short as 2 minutes gave adequate results. The cruciform pattern was used to check for any misalignment in the positioning of the coupon relative to the incident beam.
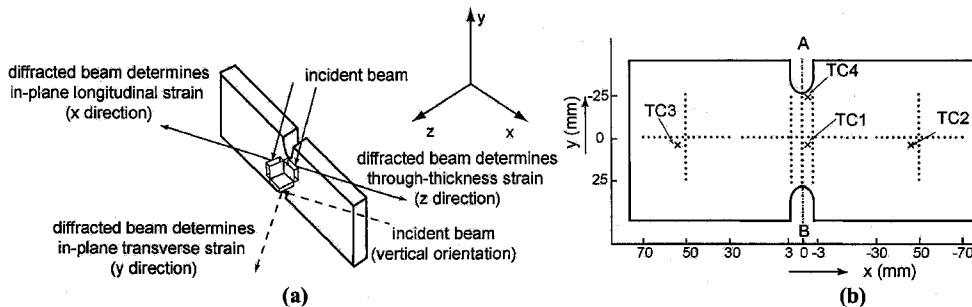
**FIGURE 2. (a)** Orientation of the coupon relative to the incident neutron beam that facilitated measurements of residual strains in the in-plane longitudinal (x), in-plane transverse (y) and through-thickness (z) directions. The irradiated volume is approximately 8 mm³. **(b)** Location of neutron diffraction measurements (dots) and placement of thermocouples (crosses) on the welded coupon. For clarity, the axes scales are not linear.

## Neutron Spectra Analysis

The diffraction spectra were analyzed by fitting the entire spectra in Rietveld refinements. The Rietveld refinement procedure [7] optimizes parameters that include atom fractions and lattice spacings until the calculated spectrum exhibits the best least squares fit to the measured spectrum. The General Structure Analysis System (GSAS) 8] code was used and incorporated reflections from planes with d-spacings between 0.5 to 2.5 Å in the face-centered cubic structure from Ref. [9]. Residual strains were calculated in the x, y and z directions from

$$\varepsilon_s = \frac{a_s - a_0}{a_0}, \tag{1}$$

where $a_s$ is the Rietveld determined lattice parameter at a distance s from the coupon center and $a_0$ is the corresponding "stress free" lattice parameter. The ends of the welded coupon were assumed to be not influenced by the weld and the "stress free" lattice parameter was determined from an average of the lattice parameter measurements at the ± 70 mm locations, at the coupon ends (see FIGURE 2b). This average lattice parameter for the welded coupon was within error when compared with lattice parameter measurements from the as-received and fatigued coupons, validating the assumption that the ends of the coupon were indeed "stress free". From the measured residual strains in the x, y and z directions, $\varepsilon_x$, $\varepsilon_y$ and $\varepsilon_z$, the corresponding residual stresses, $\sigma_x$, $\sigma_y$ and $\sigma_z$ can be computed using equations for isotropic Hookean elasticity:

$$\sigma_x = \frac{E}{1+v}[\varepsilon_x + \frac{v}{1-2v}(\varepsilon_x + \varepsilon_y + \varepsilon_z)], \tag{2}$$

$$\sigma_y = \frac{E}{1+v}[\varepsilon_y + \frac{v}{1-2v}(\varepsilon_x + \varepsilon_y + \varepsilon_z)], \tag{3}$$

171

$$\sigma_z = \frac{E}{1+\nu}[\varepsilon_z + \frac{\nu}{1-2\nu}(\varepsilon_x + \varepsilon_y + \varepsilon_z)], \tag{4}$$

where, E and $\nu$ are the Young's modulus (199 GPa) and Poisson's ratio (0.28), respectively, of the INCONEL 718 alloy [10]. The von Mises effective stresses can then be calculated, assuming that stresses in the x, y and z directions are the principal stresses, as:

$$\sigma_{eff} = \sqrt{0.5((\sigma_1 - \sigma_2)^2 + (\sigma_2 - \sigma_3)^2 + (\sigma_3 - \sigma_1)^2)}, \tag{5}$$

where, $\sigma_1$, $\sigma_2$, and $\sigma_3$ are the principal stresses.

## RESULTS AND DISCUSSION

FIGURE 3a shows the in-plane longitudinal strains ($\varepsilon_x$) measured at points along a line between the notches in the welded (RS5), as-received (RS1) and fatigued (RS3) coupons. The measurements were made with the coupons in the horizontal orientation at room temperature. Thus, the x-axis label in the figure indicates the distance from the center of the coupon along a line between the coupon notches (AB in FIGURE 2b). FIGURE 3a shows tensile strains along the welds and compressive strains in the region between the welds in the center of the welded coupon. This distribution is clearly absent in the as-received and fatigued coupons.

To confirm that the strain distribution in the welded coupon was not an artifact of lattice parameter changes due to chemistry (e.g., the introduction of filler material during the welding process or diffusion processes), FIGURE 3b is presented. FIGURE 3b compares the in-plane longitudinal strains ($\varepsilon_x$) and the through-thickness strains ($\varepsilon_z$) at room temperature, at the same locations as in FIGURE 3a. As described previously, recording neutron spectra at a given location determines the strain in both x and z directions since two banks of detectors are used. If there were changes in the lattice parameter, both curves would likely follow similar trends. On the contrary, the strain distribution in the two directions are different indicating a multi-axially distributed strain field due to the weld repair process.

FIGURE 4a shows the temperature of the welded coupon with time during the cooling
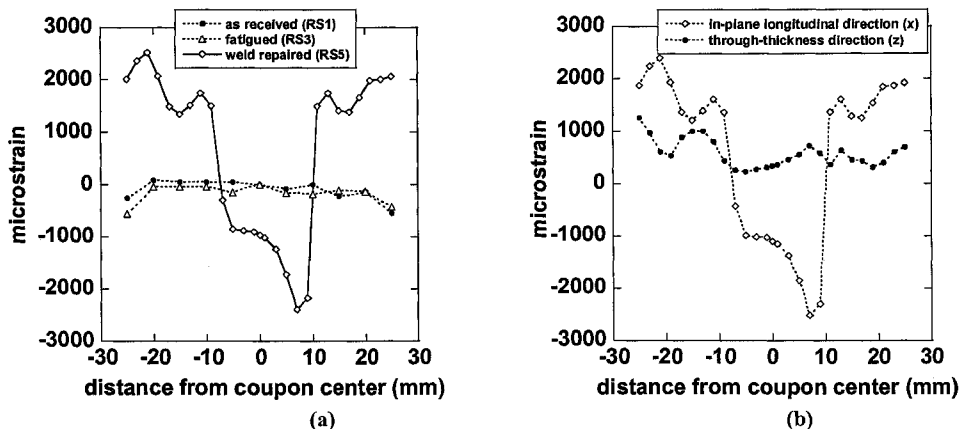


FIGURE 3. (a) Strains in the in-plane longitudinal (x) direction in the welded, as-received and fatigued coupons. (b) Strains in the in-plane longitudinal (x) and through-thickness (z) directions in the welded coupon.
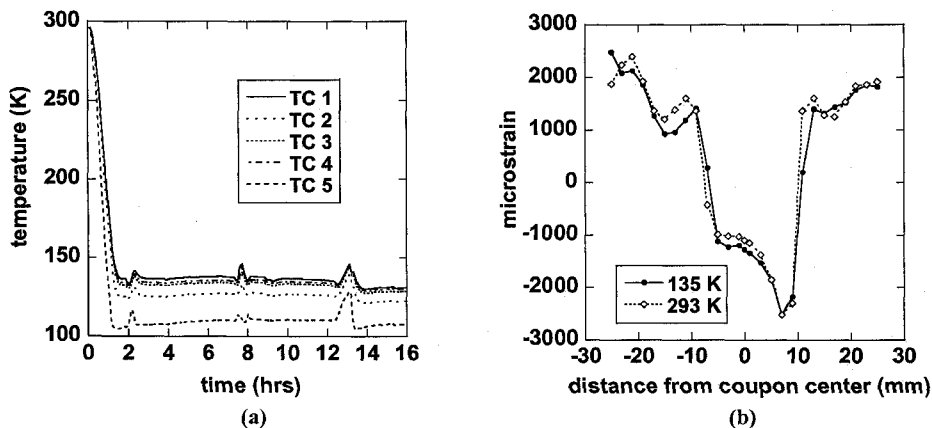
172

**FIGURE 4. (a)** Temperature of the welded coupon during cooling and neutron diffraction measurements. The locations of the thermocouples are shown in FIGURE 2b with TC5 being placed on the cold mass. The spikes represent change of dewars. **(b)** Strains in the in-plane longitudinal (x) directions in the welded coupon at 293 K and 135 K.

process in the vacuum test chamber. TC1, TC2, TC3 and TC4 were thermocouples placed on the welded coupon at locations shown in FIGURE 2b. Thermocouple TC5 was placed on the "cold mass" that cooled the coupon fixture. Visual inspection confirmed the absence of ice build-up in the chamber. After the chamber was pumped down, the center of the coupon took about 1.7 hours to cool down from 293 K to 135 K, and the temperature variation in the coupon was within ±2 K during the diffraction measurement. The temperature gradient across the sample length, i.e., from center to either end at ±70 mm varied within ± 10-20 K and was within experimental error.

FIGURE 4b compares the in-plane longitudinal strains ($\varepsilon_x$) at points along a line between the notches in the welded coupon at 293 K and 135 K. It is important to recognize that while the cooling process resulted in a thermal contraction and a concomitant decrease in the lattice parameter (not shown), the strains reported at 135 K in this figure represent lattice parameter changes relative to a stress free parameter also at 135 K that takes into account this thermal contraction. The fact that there are no substantial changes in the strain distribution suggests that differences in the coefficient of thermal expansion between the
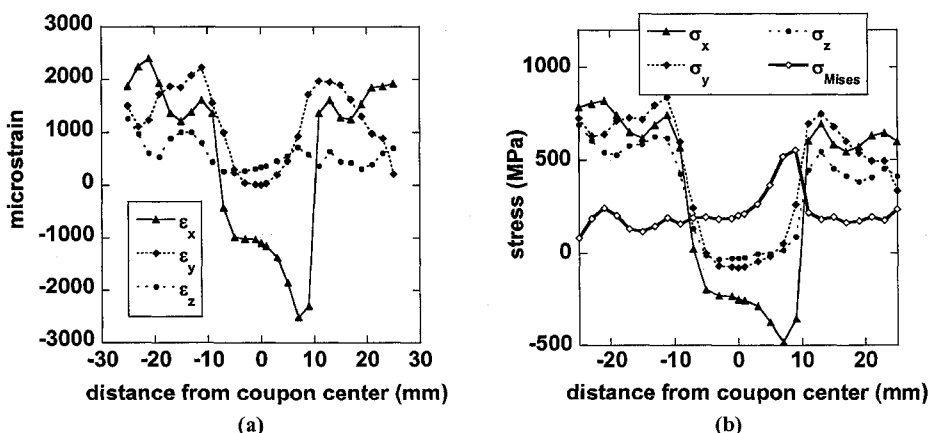


**FIGURE 5. (a)** Strains in the in-plane longitudinal (x), in-plane transverse (y) and through-thickness (z) directions. **(b)** The corresponding stresses and the von Mises effective stress determined from EQUATION 2-5.

173

weld and the base material are minimal. This is consistent with the weld repair process that did not introduce any foreign material. Furthermore, this is also consistent with our assessment of FIGURE 3b which indicated the lack of any significant chemistry effects. Such effects have the potential to change the coefficient of thermal expansion thereby introducing mismatch strains during the cooling process.

FIGURE 5a shows the in-plane transverse ($\varepsilon_y$) strains measured at points along a line between the notches in the welded coupon. The coupon was placed in the vertical orientation for this set of measurements. For direct comparison the in-plane longitudinal ($\varepsilon_x$) and through-thickness ($\varepsilon_z$) strains are also included in FIGURE 5a. The in-plane transverse ($\varepsilon_y$), in-plane longitudinal ($\varepsilon_x$) and through-thickness ($\varepsilon_z$) strains were used to determine the corresponding stresses and the Mises effective stress from EQUATIONS 2-5. On average, the Mises effective stresses are around 220 MPa but peak to about 555 MPa at the tip of the lower weld. The error associated with such measurements is typically in the 25 MPa range and is associated with experimental error as well as the statistics of the Rietveld refinement. While the yield stress of the coupon is not exactly known, it is expected to be in the range of typically aged INCONEL 718 alloys, i.e., 1100 - 1250 MPa [11]. It is not unreasonable to expect these residual stresses to influence crack growth rates in the coupons even though their effects on crack initiation thresholds or lifetime tests may be negligible (such as the weld repair certification process described earlier).

The asymmetry in the Mises stress distribution is not fully understood and may be a result of unequal crack growth at the two notches or differences in the crack and weld path from the neutron measurement profile. Furthermore, the purely tensile nature of the in-plane transverse ($\varepsilon_y$) and through-thickness ($\varepsilon_z$) strains was surprising and may be a result of a misalignment that impacted the "stress free" lattice parameter in the y and z directions. While these issues are currently being examined and accounted for in Ref. [6], using the cruciform profile measurements and other longitudinal scans not reported here, they are not expected to significantly alter the conclusions of this paper.


**CONCLUSIONS**

Neutron diffraction was used to determine residual strains in a spatially resolved mode around welds in an INCONEL 718 coupon at room temperature and at 135 K. The material and weld repair process investigated, duplicated NASA's weld repair process for cracks on the space shuttle flow liners. The following are the conclusions:
1. By measuring strains in three orthogonal directions, the weld repair process was found to introduce Mises effective residual stresses of up to 555 MPa. These stresses were confirmed to originate due to the weld repair process and are not associated with lattice parameter changes from materials chemistry effects
2. On comparing the measurements at 293 K and 135 K, no significant strains were additionally induced due to the 158 K drop in temperature. This is indicative of minimal mismatch in the coefficients of thermal expansion between the base metal and the weld.
3. The experiments demonstrated the capability of the Spectrometer for Materials Research at Temperature and Stress (SMARTS) at Los Alamos National Laboratory to perform spatially resolved measurements at cryogenic temperatures.

## ACKNOWLEDGEMENTS

## REFERENCES

1. Hutchings, M. T. and Krawitz, A. D., *Measurement of Residual and Applied Stress Using Neutron Diffraction*, Kluwer Academic, Dordrecht, The Netherlands, 1992.
2. Larsson, C., Holden, T.M., Bourke, M.A.M., Stout, M., Teague, J. and Lindgren, L.-E., Mat. Sci. Engr. A, (accepted 2003).
3. Bourke, M. A. M., Dunand, D. C. and Üstündag, E., App. Phy. A: Mat. Sci. Process. **74** No. 6, 1707-1709 (2002).
4. Livescu, V., Woodruff, T., Clausen, B., Bourke, M.A.M., Notardonato, W.U. and Vaidyanathan, R., "Design and Rationale for in situ Cryogenic Deformation Capability at a Neutron Source", submitted for publication in Advances in Cryogenic Engineering, 2003.
5. Woodruff, T.R., Masters Thesis, "Development of a Cryogenic Testing Capability on the Spectrometer for Materials Research at Temperature and Stress", University of Central Florida, 2004.
6. Rathod, C.R., Livescu, V., Clausen, B., Bourke, M.A.M., Notardonato, W.U., Femminineo, M. and Vaidyanathan, R., "Determination of Residual Stresses in a Welded INCONEL 718 Coupon at Cryogenic Temperatures", to be submitted to Acta Materialia.
7. Von Dreele, R. B., *J. Appl. Crystallogr.* **30**, 517-525 (1997).
8. Larson, A. C. and Von Dreele, R. B. *General Structure Analysis System (GSAS)*, Los Alamos Report No. LAUR 8-748, Los Alamos National Laboratory, Los Alamos, NM (1986).
9. Szytula, A and Leciejewicz, J, *Handbook of crystal structures and magnetic properties of rare earth intermetallics,* Boca Raton, Fla.: CRC Press, 1994.
10. Special Metal Corporation, New Hartford, New York, USA.
11. Reed, R.P. and Clark, A.F., *Materials at Low Temperatures*, ASM, Metals Park, Ohio, 1983, pp.404-405.